Visualising Excitations at Buried Heterojunctions in Organic Semiconductor Blends

Andreas C. Jakowetz[1], *Marcus L. Böhm*[1], *Aditya Sadhanala*[1], *Sven Huettner*[2], *Akshay Rao**[1] *and Richard H. Friend**[1]

[1] Cavendish Laboratory, Department of Physics, University of Cambridge, J J Thomson Avenue, Cambridge, CB3 0HE, United Kingdom

[2] Fakultät für Biologie, Chemie und Geowissenschaften, University Bayreuth, Universitätsstrasse 30, 95440 Bayreuth, Germany

e-mail: ar525@cam.ac.uk, rhf10@cam.ac.uk

KEYWORDS: Interface, Disorder, Charge Generation, Driving Energy, Ultrafast Spectroscopy, Transient Absorption, Pump-Push, SAXS, WAXS, PDS, Polymer, Fullerene, Organic Photovoltaics

Abstract:

Interfaces play a crucial role in semiconductor devices, but in many device architectures they are nanostructured, disordered, and buried away from the surface of the sample. Conventional optical, X-ray and photoelectron probes often fail to provide interface-specific information in such systems. Here we develop an all-optical time-resolved method to probe the local energetic landscape and electronic dynamics at such interfaces, based on the Stark effect caused by electron-hole pairs photo-generated across the interface. Using this method, we found that the electronically active sites at the polymer-fullerene interfaces in model bulk-heterojunction blends fall within the low-energy tail of the absorption spectrum. This suggests that these sites are highly ordered compared to the bulk of the polymer film, leading to large wavefunction delocalisation and low site energies. We also detected a 100fs migration of holes from higher to lower energy sites, consistent with these charges moving ballistically into more ordered polymer regions. This ultrafast charge motion may be key to separating electron-hole pairs into free charges against the Coulomb interaction.

Understanding the properties of nanoscale and disordered interfaces presents a critical scientific challenge, cutting across the areas of condensed-matter physics, materials science, physical chemistry, and biology. A range of techniques, such as atomic resolution electron microscopy, photoelectron, and X-ray measurements, has been used to probe the properties of conventional 'ordered' interfaces, such as those in inorganic semiconductor or magnetic heterostructures.[1] Yet, these techniques have proved extremely challenging to apply directly to nanoscale and disordered interfaces which are often buried away from the surface of the sample. This means that conventional optical, photoelectron or X-ray techniques are often swamped by signal from the 'bulk' of the samples and not sensitive to the interface. Interface specific techniques, such as sum-frequency generation (SFG), require well defined and sharp interfaces in order to generate signal, which makes them unsuited to the disordered and often random morphologies of these interfaces.[2]

Bulk-heterojunctions (BHJs) between organic semiconductors, which comprise an intermixed blend of p- and n-type semiconductor[3–8], provide a model disordered nanoscale interface. The electronic structure and disorder at and near (<5 nm from) these interfaces controls wavefunction delocalisation, charge transfer, separation and recombination efficiency and thus the performance of optoelectronic devices, such as organic photovoltaics (OPVs) and organic light emitting diodes (OLEDs).[9–11] A tremendous amount of work has been done to understand the physical and chemical structure of these interfaces.[12,13] Yet, to date no techniques exist that can report directly on the dynamics of populated electronic states at and near these buried interfaces.

Here, we demonstrate an all-optical method to access information on the electronic properties of such buried and disordered interfaces and their neighbouring electronic sites, and use it to study model BHJ OPV polymer-fullerene blends. We utilise an ultrafast pump-push-probe

technique which measures the quadratic Stark effect caused by electron-hole pairs generated across the interface between n- and p-type semiconductors. This "electroabsorption" signal provides a unique signature of the dynamics of electronic states in the interfacial region, allowing us to precisely map the local energetic landscape that the charges sample as they move away from the interface. Very surprisingly, we find firstly that the local bandgap of the electronically active interfacial sites is strongly redshifted compared to the bulk and secondly, that charges can move from higher-energy to low-energy regions on sub 100fs timescales, consistent with ballistic motion of holes.

As model system we use the polymer donor [N-11"-henicosanyl-2,7-carbazole-alt-5,5-(4',7'-di-2-thienyl-2',1',3'-benzothiadiazole)] (PCDTBT) which is blended with one of the Phenyl-C_{61}-butyric acid methyl ester derivatives mono-$PC_{61}BM$ (mPCBM), bis-$PC_{61}BM$ (bPCBM), and tris-$PC_{61}BM$ (tPCBM). Weight ratios between polymer and fullerene are 1:1 across the set of fullerenes and 4:1, 1:1, and 1:4 for PCDTBT:mPCBM blends. The chemical structure of the materials can be found in Figure 1 (a). UV-Vis and photoluminescence (PL) spectra for PCDTBT and mono-PCBM, can be found in Figure S1.1. The internal quantum efficiency of optimised (1:4) PCDTBT:mPCBM blends is close to 100%[14]. The system has been previously well characterised optically and structurally.[15–18] For instance several studies have shown that structurally all blends consist of intermixed regions of fullerene and polymer, the so-called mixed-phase.[12,13] Intercalation of fullerenes between the amorphous PCDTBT chains is observed[19–21] and strong similarities to fullerenes intercalating in-between MDMO-PPV are reported.[19,22] Adding more fullerene leads to complete filling of the intercalated sites and eventually results in pure fullerene domains, this allows for a controlled comparison of charge separation and the formation of charge transfer states through the variation of fullerene content.[23] The addition of side groups to the fullerenes leads to increased disorder in the packing, as has been discussed previously. This is confirmed by small-/wide-angle X-

ray scattering (SAXS/WAXS) spectra of the different materials and compositions, which showed that mono-adduct fullerenes form the largest aggregates, while adding more side groups lowers aggregate size (see Section S2). Furthermore, increasing fullerene content leads to larger aggregate size, which leads to formation of larger networks within the fullerene domain.[24] Increased disorder in the fullerene phase has been linked to inefficient charge generation, higher charge recombination and poor device performance.[25] Thus the wide tunabilty of the system via the choice and amount of fullerene added made PCDTBT an ideal system to elucidate the role of structure on electronic dynamics. However, the exact energetic landscape at the interface and effect of the fullerene phase on the packing of the polymer and how this influences charge dynamics are difficult to quantify due to lack of suitable interface specific probes.

Time-resolved optical pump-probe spectroscopies provide powerful ways to study the electronic properties of such systems.[26] In these methods, a laser pulse excites the sample, generating excitations such as charges and excitons. Sometime later, a probe pulse interrogates the sample and measures the change in absorption (transmission) induced by the pump pulse. Excited states generated by the pump pulse correlate directly to a lower ground-state population and will thereby lead to a ground-state bleach (GSB) in absorption. While initial excitations can contribute to the overall signal with stimulated emission (SE) due to their singlet character, all excited states have a photo-induced absorption (PIA) feature, the spectral shape of which depends on the material and the nature of the excited state. Importantly, pump-probe methods provide information on the specific site/chromophore on which the excitation is when probed, but not on the surrounding sites. Furthermore, these techniques do not provide any interface specificity, rather they provide information of whichever site/chromophore the excitation is located on.

Turning to the case of interfaces, we find that pump-probe spectroscopy can provide additional information. As illustrated in Figure 1 (c), when excitons are dissociated at the interface between p- and n-type semiconductors, they form electron-hole (e-h) pairs which act as a local electric dipole and induce a quadratic Stark shift on the energy levels of the surrounding molecules. The Stark shift causes a change in the absorption spectra of the surrounding molecules, normally leading to a redshift in absorption due to lowering of optical absorption gap. The difference between the two absorption spectra (with and without electric field), takes the form of a derivative of the absorption spectra and is conventionally referred to as electroabsorption (EA).[27] This is illustrated in the cartoon in Figure 1(b). Thus, pump-probe spectroscopy of interfaces contains a mix of GSB, PIA, SE and EA signals, as illustrated in the lower panel of Figure 1(c).

This EA signal has been used to create powerful pump-probe methods to investigate the interfaces of inorganic and organic material systems.[11,28–30] Recently, we have demonstrated that this EA can be tracked as a function of time at BHJ interfaces. As the e-h pair separates across the interface, the electric field associated with it varies, giving rise to a time-dependent electric field and hence a time-dependent Stark shift and EA signal. By monitoring the dynamics of the EA signal it is possible to track the separation of e-h pairs on fs timescales.[11] Using this method it was shown that for the PCDTBT:PCBM (1:4) system, charge separation occurs on a sub 100fs timescale, which was attributed to ballistic motion of the electrons through fullerene clusters.[11] Furthermore, using an EA signal, it has been shown that also polarons in a pBTTT:PCBM system can move on timescales <1ps between different phases of the BHJ, i.e. from a co-crystal region to domains of pure pBTTT.[29]

But the EA signal also contains information about the molecules which are affected by the electric field of the separating e-h pair, as illustrated in the cartoon in Figure 1 (c).

Importantly, these molecules must lie at or near the interface between n- and p-type semiconductors. The observed EA signal resembles the first derivative of the absorption spectra of these molecules (see more details in the SI, Section S4), as reported in the literature on TA measurements[11,29,30] and steady-state EA experiments[31]. Integrating this over photon energy gives the ground state absorption spectra of these molecules. Thus, the EA signal could provide us a window on the energetic landscape experienced by charges as they move away from the interface. However, extracting pure EA signatures from pump-probe data is very difficult due to overlapping spectral signatures and energy relaxation (see Section S3.2).[16] Such signals also contain information from all the molecules influenced by the electric field, and this reduces the spatial resolution of the information we can obtain.

We present here a new pump-push-probe electroabsorption (PPP) technique, which uses a third 'push' pulse in order to obtain clean EA signatures on more localised areas. In this technique, the above-gap pump pulse creates a population of singlet excitons on the donor. After electron transfer, e-h pairs are created across the donor-acceptor interface. We follow this with a time-delayed 'push' pulse, at 2000nm (0.62eV), which is targeted in the low-energy PIA of the hole-polarons. Previously, it has been shown that this push pulse excites hole-polarons within their electronic manifold, briefly delocalising them. The holes will rapidly relax and localize on sub 200fs timescales, but some of them would have moved onto adjacent polymer chains.[9] Thus in our experiment, the push pulse acts as an optical method to move the hole-polaron. We note that the wavelength of the push pulse is chosen to be in a background free region where it does not overlap with absorptions from singlet or triplet exciton on the polymer, or charge transfer states, nor does it directly generate excitations on the polymer, as it is well below the bandgap. Importantly, as we report here, by moving the hole we change the electric field distribution caused by the e-h pair, as illustrated in Figure 1 (d). The PPP signal thus contains a mix of GSB, PIA, SE and a modified EA signal. By

alternating the excitation sequence of the sample between pump-push and pump-only laser pulses, we are able to obtain a very clean subtraction of the pump-only signal from the pump-push signal. This leaves only the difference between the two EA signals (with and without push). As illustrated in Figure 1 (e), this EA signal reports only on the small subset of molecules brought into, or removed from, the influence of the electric field by the movement of the charge following the push pulse. As it is the hole polaron that is being pushed within the experiment, the change observed will come mostly from the movement of the hole within the polymer phase. This allows us to monitor just a small spatial volume around the hole-polaron, providing a nanoscale window into the energetic landscape near the interface and to trace it while it moves away from the interface towards the bulk. Thus, the experimental method presented here has analogies with super-resolution STED microscopy, in the use of a switching methodology (here by the use of the push pulse) to achieve a high spatial resolution.

For the sake of clarity, in the following text we focus our investigation on 4:1 and 1:4 for PCDTBT:mPCBM blends. The 1:4 blend provides best solar cell operation, with quantum yields for charge collection close to 100%[14] and the 4:1 blend provides a comparison as a system with efficient early time electron-hole pair generation but inefficient long-range charge separation. Also, both blends are on the extreme ends of the ordered and disordered scale. Data for others blends, which show similar trends to those discussed in the main text, are provided in the SI (see Section S3.3.1).

Figure 2(a) shows the map of PCDTBT:mono-PCBM (4:1) for excitation with both pump and push pulses. The sample is excited at 0 ps with a 500 nm pump pulse and pushed after 4.9 ps with a 2000 nm infrared pulse. Figure 2(b), shows the final map produced by the pump-push-probe experiment which gives only the differential signal induced by the push pulse. It can be

186 seen that the push pulse induces both a positive and a negative feature. We note that the zero-
187 crossing, i.e. the transition point from positive to negative signals, in this map is at higher
188 energies (roughly at 600 nm) compared to the normal pump-probe one (at around 650 nm),
189 indicating that the signal is not related to an increased excited state population (see more
190 details in the SI, Section S4).
191
192 The main spectral component of the pump-push response, as revealed by a global analysis on
193 the data, is shown in Figure 2(c). This feature is found to be well matched well with the
194 steady-state EA spectrum, shown by the dotted line, which has been measured previously.[11]
195 Thus, we find that the push pulse gives rise to an EA signal, as described above, which
196 contains information on the molecules near the interface. We note that spectra taken from the
197 raw data show the same trend (see Figure S3.5). However, the global analysis yields cleaner
198 spectral signatures, more details on this can be found in the SI (Section S5).
199
200 Figure 3(a) summarises the EA spectra obtained for the 4:1 and 1:4 for PCDTBT:mPCBM
201 blends (data on other blends can be found in the SI, Figure S3.3). As described above, due to
202 the derivative nature of the EA signal, integration yields the underlying absorption spectra of
203 the molecules at and near the interface affected by the electric field of the e-h pair (as
204 illustrated in Figure 1(e)). These interfacial absorption spectra are shown in Figure 3(b). We
205 observe that for both blends the interfacial absorption is significantly red-shifted compared to
206 the bulk of the polymer film (green dashed line, integration of CW EA of a
207 PCDTBT:mPCBM film). This cannot be explained by the UV-Vis spectra of blends, that are
208 only slightly red-shifted compared to the neat polymer (see Figure S1.2). Figure 3(c) shows
209 the absorption spectra of the neat polymer film measured with photothermal deflection
210 spectroscopy (PDS), which provides several orders of magnitude in detection sensitivity in
211 absorption and is not distorted by reflection and scattering.[32] It can be seen that the interfacial

absorption measured via the PPP technique lies in the low-energy tail of the neat polymer film, whose absorption is two orders of magnitude below the absorption peak. This means that the polymer chains that make up the electronically active interfacial sites represent a very small fraction (<1%) of the total chains in the film. We consider that the very low energy of these electronically active interfacial sites must be related to highly planar and ordered polymer backbones, leading to larger wavefunction delocalisation and low bandgaps. This suggests that in all the blends studied here, the electronic dynamics at the interface are controlled by a very small fraction of sites (which are not representative of the bulk film) which are highly ordered, planar, and of lower energy than the bulk of the polymer film.

The widths of the absorption spectra are listed next to the legend in Figure 3(b) and correspond to the FWHM of a modified bi-Gaussian fit to the respective curve. The width of the obtained curves exhibits the same trend as the SAXS/WAXS results (see Section S2), which can be seen in the fullerene and polymer scattering peaks, indicating that order in one phase influences the other and therefore higher order of the fullerene leads to a more highly ordered polymer, i.e. increased fullerene content and better fullerene packing lead to increased order in the polymer phase near the interface. This ordering effect has been reported in the literature for the amorphous polymers PCDTBT and MDMO-PPV upon fullerene addition.[19,22,33,34]

We have also found similar trends of the EA feature using PCDTBT blended with a range of other fullerene derivatives: mPCBM, bPCBM, and tPCBM, as reported in the SI (Section S3.3.1). Here, for 1:1 blends the sample with tPCBM exhibits the strongest blue-shift and the highest FWHM value for the integrated EA spectrum, in good agreement with the largest disorder of PCDTBT:tPCBM. With decreasing disorder towards bPCBM and mPCBM, the spectra get further red-shifted and narrower. Furthermore, we find that pushing either the low

238 or higher-energy polaron PIA using 2000 nm or 1200 nm, respectively, both yields the same
239 trend across blend disorder (see Figure S3.6). Using the 1200 nm push, blue and red-shifts
240 get even more pronounced across the disorder series which could be related to a larger
241 induced e-h distance and hence sampling a larger material volume.
242
243 The analysis above was performed for measurements in which the 2000 nm push pulse
244 arrives 0.9 ps after the pump pulse. But by varying the time delay between pump and push
245 pulses, we can monitor the differential EA signal as a function of time, as the e-h pairs
246 separate and move away from the interface. This allows us to track the local environment
247 experienced by the e-h pairs as a function of time.
248
249 Figure 4(a) shows integrated the EA spectra at different push times for the
250 PCDTBT:mPCBM (4:1) blend. This ratio of polymer to fullerene gives rise to a blend in
251 which fullerene are well dispersed within the polymer side chains and there are very few
252 fullerene aggregates.[20,35] Though exciton dissociation is efficient in this blend, it does not
253 give rise to long-range charge separation and shows low external quantum efficiencies (EQE)
254 in OPV devices.[11] As shown in Figure 4(a), the spectra for the earliest time slices are the
255 most red-shifted and blue-shift over time. This suggests that for the PCDTBT:mPCBM (4:1)
256 blend, hole polarons are formed within lower-energy regions, where the polymer is relatively
257 better ordered (leading to a red-shifted signal in Figure 4(a)), and then on picosecond
258 timescales move into higher-energy more disordered regions, which more closely resemble
259 the bulk of the polymer phase. Figure 4(c) shows this shifting of the peak as a function of
260 time. This need to move from lower energy to higher energy areas, as charges move away
261 from the interface, is clearly an energetically unfavourable configuration for long-range
262 charge separation. This is consistent with the poor long-range charge separation and EQE and
263 high geminate recombination in these blends.

In contrast, the PCDTBT:mPCBM (1:4) blend shows fullerene aggregates, gives rapid long-range charge separation and excellent EQE in devices.[11] As shown in Figure 4(b) the spectrum initially red-shifts strongly over the first 150 fs before blue-shifting over the next 1 ps. The shifting of the peak position is shown in Figure 4(c). This suggests that charges are initially located in more disordered regions and rapidly move into regions with higher order within the first 150 fs. Such motion of charges from disordered to ordered regions is consistent with a model of the system in which charges are generated in a disordered mixed phase and then move into more ordered regions, lowering their energy while doing so. However, the timescale for this movement into ordered regions, 150 fs, suggests that charges are moving extremely rapidly at early times. Indeed, such fast timescales are inconsistent with incoherent charge hopping, but are consistent with previous observations of ballistic charge separation in the PCDTBT:mPCBM (1:4) blend, attributed to ballistic motion of electrons through fullerene clusters.[11] The results here suggest that the hole polaron also moves very rapidly on early time scales, exploring the local energetic landscape on 150 fs timescales and moving towards low energy, better ordered sites away from the interface. This early time motion allows the e-h pair to overcome the Coulomb barrier on sub 200 fs timescales with high efficiency. As a result, this blend ratio shows very little geminate recombination.[9,16]

At later times, the charges then slowly move back into more disordered polymer regions on ps timescales, as they move away from the interface and into the bulk of the polymer. However, since e-h separation beyond the Coulomb capture range (considered to be 5 nm[11]) was achieved at early times, this later time, energetically unfavourable motion does not seem to hinder device performance. We also note, that having interfacial sites that are higher energy than neighbouring sites adjacent to the interface would also prevent charges from

290 moving towards the interface at longer timescales, acting as a barrier to longer time non-
291 geminate recombination.
292
293 Our results reveal that, very surprisingly, in polymer-fullerene blends the electronically active
294 interfacial sites lie in the low-energy tail of the neat polymer film, forming a very small
295 subset of the total chains in the film. These low energy sites are most likely highly planar and
296 ordered polymer chains, which enables larger wavefunction delocalisation and low bandgaps.
297 We note that these sites are different from CT states which exhibit transitions at much lower
298 energies of around 1.46 eV (see Figure S1.1).[17] In unoptimised 4:1 polymer:fullerene blends,
299 charges are formed at the lowest energy sites, and moving away from the interface entails an
300 energetic penalty, leading to low EQEs and high geminate recombination. For the optimised
301 1:4 polymer:fullerene blend the interfacial energetics drive a very rapid, sub 150fs, motion of
302 hole polarons away from the higher energy interfacial sites to low energy more highly
303 ordered sites. This rapid motion helps to overcome the Coulomb interaction and is consistent
304 with early time ballistic charge transport. Thus, the energetic structure of the interface and the
305 regions adjacent to it, are key to understanding both the poor EQEs of the 4:1 polymer-
306 fullerene blend as well as the very high EQEs in the 1:4 blend. This new all-optical method
307 developed here provides a unique window on the molecular ordering and energetic landscape
308 and electronic dynamics of interfacial sites. The technique is a straightforward modification
309 of the widely used technique of optical pump-probe spectroscopy and can readily be extended
310 to other disordered, buried semiconductor interfaces across which electron-hole pairs can be
311 generated. This may include interfaces such as organic/metal-oxides[36], organic/perovskite[37],
312 organic/colloidal quantum dots (CQD)[38,39], CQD/CQD heterojunctions[40], and CQD/metal-
313 oxide junctions[40].
314

315 **Methods:**

316 **Sample preparation:**

317 PCDTBT was purchased from 1-material, PCBM, bis-PCBM, tris-PCBM were purchased
318 from Solenne BV. All materials were used as received.

319 Polymer:fullerene blends were spun from ortho-dichlorobenzene with 10 mg/ml for 4:1, and
320 1:1 blends (polymer:fullerene mass ratio) and 15 mg/ml for 1:4 blends, respectively. Films
321 were prepared on ultrathin glass substrates (130 µm) which were cleaned by sonication in
322 acetone and isopropyl alcohol and exposure to O_2 plasma for 10 min each. Substrates were
323 subsequently brought in an oxygen and water free glovebox (O_2 < 5 ppm, H_2O < 1 ppm) and
324 spun at 1500 RPM for 120 s. Films were encapsulated in the glovebox using microscope
325 cover slides as spacer between film and second ultrathin cover glass, sealing the edges with
326 epoxy resin.

327

328 **Ultrafast Transient Absorption Spectroscopy (TA):**

329 Transient Absorption spectra were acquired using a 1 kHz regenerative Ti:Sapphire amplifier
330 (Solstice, Spectra-Physics), seeding two homebuilt broadband non-collinear optical
331 parametric amplifiers (NOPAs). One NOPA was used as a broadband visible probe while the
332 other NOPA was used as the pump source, tuned to 500 nm pulses with 9 µJ/cm² (1200 nm
333 push) and 40 µJ/cm² (2000 nm push) pulse energy, respectively, after compression using a
334 pair of dielectric chirped mirrors (Layertec 109811) and chopped at 500 Hz. The probe light
335 was split into two separate beams, one probe and one reference beam. Both got dispersed
336 with a grating spectrometer (Shamrock SR-303i, Andor Technology) and measured
337 simultaneously with a CCD detector array each (Entwicklungsbüro Stresing). Here, the
338 reference is not subject to the pump beam and is therefore used to correct for shot-to-shot
339 fluctuations in the system.

For pump-push-probe measurements, we used the TA setup described above and a commercial OPA (TOPAS, Light-Conversion) to create the infrared push pulse of 2000 nm at 25 mJ/cm² and 1200 nm at 3 mJ/cm² for the respective experiments, chopped at 250 Hz. The wavelengths of the push are tuned to the low energy edge of the respective polaron PIA bands (Figure S3.1). The high fluence of the push pulse is needed due to the low absorption cross-section of the excited states in this spectral region. Mathematical processing of the acquired data is described in Section S3.3.3 and more details on the global analysis can be found in Section S5. Each of the presented data curves is the result of an average over 8 individual global analysis fits per dataset.

Wide / Small Angle X-ray Scattering (WAXS / SAXS):

The WAXS/SAXS characterization has been performed according to previous works (ref.41) and reproduced here for completeness: Combined SAXS and WAXS measurements of the bulk material were carried out at the SAXS beamline of the Australian Synchrotron using a Pilatus 1M and a Pilatus 200k detector. The beam energy and detector distances were chosen in such a way, that there was a small overlap between the SAXS and WAXS signal, so that the resulting curves could be stitched together at $q = 0.73$ Å^{-1}.

Photothermal Deflection Spectroscopy (PDS):

The PDS sample was prepared by spin-coating PCDTBT from 10 mg/ml solution in ortho-dichlorobenzene on water free quartz substrates (Spectrosil).

The experiment has been carried out as reported in previous works (ref.42) and is reproduced here for completeness: PDS is a scatter-free surface sensitive absorption measurement capable of measuring 5-6 orders of magnitude weaker absorbance than the band edge absorption.

For the measurements, a monochromatic pump light beam is shined on the sample which on absorption produces a thermal gradient near the sample surface via non-radiative relaxation induced heating. This results in a refractive index gradient in the area surrounding the sample surface. This refractive index gradient is further enhanced by immersing the sample in an inert liquid FC-72 Fluorinert® (3M Company) which has a high refractive index change per unit change in temperature. A fixed wavelength CW laser probe beam is passed through this refractive index gradient producing a deflection proportional to the absorbed light at that particular wavelength, which is detected by a photo-diode and lock-in amplifier combination. Scanning through different wavelengths gives us the complete absorption spectra. Because this technique makes use of the non-radiative relaxation processes in the sample, makes it immune to optical effects like interference and scattering.

Data availability:

The datasets generated during and/or analysed during the current study are available in the University of Cambridge data repository at https://doi.org/10.17863/CAM.6924.

Acknowledgements:

We would like to thank S. Gélinas, N. Paul, and F. Deschler for fruitful discussions. This work was supported by the Engineering and Physical Sciences Research Council (EPSRC) and the Winton Programme for the Physics of Sustainability. A.C.J. thanks the University of Cambridge for funding (CHESS). Synchrotron measurements were undertaken on the SAXS beamline at the Australian Synchrotron, Victoria, Australia and we acknowledge the help of Niraj Lal with the measurements. S.H. thanks the framework project Soltech for funding.

Author Contributions:

A.C.J. performed the pump-push-probe measurements, M.L.B. and S.H. performed the SAXS/WAXS experiments, A.S. conducted the PDS measurement. A.C.J., M.L.B., A.S., and S.H. analysed the data. A.R. and R.H.F. supervised the work. A.C.J., A.R., and R.H.F. wrote the manuscript. All authors commented on the manuscript.

References:

1. Agostini, G. & Lamberti, C. *Characterization of Semiconductor Heterostructures and Nanostructures (Second Edition)*. (2013).
2. Geiger, F. M. Second Harmonic Generation, Sum Frequency Generation, and $\chi(3)$: Dissecting Environmental Interfaces with a Nonlinear Optical Swiss Army Knife. *Annu. Rev. Phys. Chem.* **60,** 61–83 (2009).
3. Tang, C. W. Two-layer organic photovoltaic cell. *Appl. Phys. Lett.* **48,** 183–185 (1986).
4. Halls, J. J. M. *et al.* Efficient photodiodes from interpenetrating polymer networks. *Nature* **376,** 498–500 (1995).
5. Yu, G. & Heeger, A. J. Charge separation and photovoltaic conversion in polymer composites with internal donor/acceptor heterojunctions. *J. Appl. Phys.* **78,** 4510–4515 (1995).
6. He, X. *et al.* Formation of Nanopatterned Polymer Blends in Photovoltaic Devices. *Nano Lett.* **10,** 1302–7 (2010).
7. He, X. *et al.* Formation of Well-Ordered Heterojunctions in Polymer:PCBM Photovoltaic Devices. *Adv. Funct. Mater.* **21,** 139–146 (2011).
8. Pfadler, T. *et al.* Influence of Interfacial Area on Exciton Separation and Polaron Recombination in Nanostructured Bilayer All-Polymer Solar Cells. *ACS Nano* **8,** 12397–12409 (2014).
9. Bakulin, A. A. *et al.* The Role of Driving Energy and Delocalized States for Charge Separation in Organic Semiconductors. *Science* **335,** 1340–1344 (2012).
10. Rao, A. *et al.* The role of spin in the kinetic control of recombination in organic photovoltaics. *Nature* 6–11 (2013). doi:10.1038/nature12339
11. Gelinas, S. *et al.* Ultrafast Long-Range Charge Separation in Organic Semiconductor Photovoltaic Diodes. *Science* **343,** 512–516 (2014).

12. Kouijzer, S. *et al.* Predicting Morphologies of Solution Processed Polymer:Fullerene Blends. *J. Am. Chem. Soc.* **135,** 12057–12067 (2013).

13. Huang, Y., Kramer, E. J., Heeger, A. J. & Bazan, G. C. Bulk Heterojunction Solar Cells: Morphology and Performance Relationships. *Chem. Rev.* **114,** 7006–7043 (2014).

14. Park, S. H. *et al.* Bulk heterojunction solar cells with internal quantum efficiency approaching 100%. *Nat. Photonics* **3,** 297–302 (2009).

15. Banerji, N., Cowan, S., Leclerc, M., Vauthey, E. & Heeger, A. J. Exciton Formation, Relaxation, and Decay in PCDTBT. *J. Am. Chem. Soc.* 17459–17470 (2010). doi:10.1021/ja105290e

16. Etzold, F. *et al.* Ultrafast Exciton Dissociation Followed by Nongeminate Charge Recombination in PCDTBT:PCBM Photovoltaic Blends. *J. Am. Chem. Soc.* **133,** 9469–79 (2011).

17. Provencher, F. *et al.* Slow geminate-charge-pair recombination dynamics at polymer: Fullerene heterojunctions in efficient organic solar cells. *J. Polym. Sci. Part B Polym. Phys.* **50,** 1395–1404 (2012).

18. Provencher, F. *et al.* Direct observation of ultrafast long-range charge separation at polymer-fullerene heterojunctions. *Nat. Commun.* **5,** 4288 (2014).

19. Beiley, Z. M. *et al.* Morphology-Dependent Trap Formation in High Performance Polymer Bulk Heterojunction Solar Cells. *Adv. Energy Mater.* **1,** 954–962 (2011).

20. Cates Miller, N. *et al.* Molecular Packing and Solar Cell Performance in Blends of Polymers with a Bisadduct Fullerene. *Nano Lett.* **12,** 1566–70 (2012).

21. Cates Miller, N. *et al.* Factors Governing Intercalation of Fullerenes and Other Small Molecules Between the Side Chains of Semiconducting Polymers Used in Solar Cells. *Adv. Energy Mater.* **2,** 1208–1217 (2012).

22. Cates, N. C., Gysel, R., Dahl, J. E. P., Sellinger, A. & McGehee, M. D. Effects of

Intercalation on the Hole Mobility of Amorphous Semiconducting Polymer Blends. *Chem. Mater.* **22,** 3543–3548 (2010).

23. Jakowetz, A. C. *et al.* What Controls the Rate of Ultrafast Charge Transfer and Charge Separation Efficiency in Organic Photovoltaic Blends. *J. Am. Chem. Soc.* **138,** 11672–11679 (2016).

24. Savoie, B. M. *et al.* Mesoscale molecular network formation in amorphous organic materials. *Proc. Natl. Acad. Sci. U. S. A.* **111,** 10055–10060 (2014).

25. Savoie, B. M., Jackson, N. E., Chen, L. X., Marks, T. J. & Ratner, M. A. Mesoscopic features of charge generation in organic semiconductors. *Acc. Chem. Res.* **47,** 3385–3394 (2014).

26. Cabanillas-Gonzalez, J., Grancini, G. & Lanzani, G. Pump-probe spectroscopy in organic semiconductors: monitoring fundamental processes of relevance in optoelectronics. *Adv. Mater.* **23,** 5468–85 (2011).

27. Sebastian, L., Weiser, G. & Bässler, H. Charge transfer transitions in solid tetracene and pentacene studied by electroabsorption. *Chem. Phys.* **61,** 125–135 (1981).

28. Yang, Y. *et al.* Semiconductor interfacial carrier dynamics via photoinduced electric fields. *Science* **350,** 1061 LP-1065 (2015).

29. Scarongella, M. *et al.* A Close Look at Charge Generation in Polymer:Fullerene Blends with Microstructure Control. *J. Am. Chem. Soc.* **137,** 2908–2918 (2015).

30. De Jonghe-Risse, J. *et al.* Using the Stark effect to understand charge generation in organic solar cells. in *Proc. of SPIE* (eds. Hayes, S. C. & Bittner, E. R.) **9549,** 95490J (2015).

31. Tsutsumi, J., Yamada, T. & Hasegawa, T. Electroabsorption Study of Charge-Transfer Excited State in Donor-Acceptor-Type Polymer. *Trans. Mater. Res. Soc. Japan* **39,** 217–219 (2014).

32. Sadhanala, A. *et al.* Preparation of Single-Phase Films of CH_3NH_3 $Pb(I_{1-x}Br_x)_3$ with

473 Sharp Optical Band Edges. *J. Phys. Chem. Lett.* **5,** 2501–2505 (2014).
474 33. Melzer, C., Koop, E. J., Mihailetchi, V. D. & Blom, P. W. M. Hole Transport in
475 Poly(phenylene vinylene)/Methanofullerene Bulk-Heterojunction Solar Cells. *Adv.*
476 *Funct. Mater.* **14,** 865–870 (2004).
477 34. Tuladhar, S. M. *et al.* Ambipolar Charge Transport in Films of Methanofullerene and
478 Poly(phenylenevinylene)/Methanofullerene Blends. *Adv. Funct. Mater.* **15,** 1171–1182
479 (2005).
480 35. Mayer, A. C. *et al.* Bimolecular Crystals of Fullerenes in Conjugated Polymers and the
481 Implications of Molecular Mixing for Solar Cells. *Adv. Funct. Mater.* **19,** 1173–1179
482 (2009).
483 36. Greiner, M. T. & Lu, Z.-H. Thin-film metal oxides in organic semiconductor devices:
484 their electronic structures, work functions and interfaces. *NPG Asia Mater* **5,** e55
485 (2013).
486 37. Stranks, S. D. & Snaith, H. J. Metal-halide perovskites for photovoltaic and light-
487 emitting devices. *Nat Nano* **10,** 391–402 (2015).
488 38. Morgenstern, F. S. F. *et al.* Ultrafast Charge- and Energy-Transfer Dynamics in
489 Conjugated Polymer: Cadmium Selenide Nanocrystal Blends. *ACS Nano* **8,** 1647–
490 1654 (2014).
491 39. Böhm, M. L. *et al.* The Influence of Nanocrystal Aggregates on Photovoltaic
492 Performance in Nanocrystal-Polymer Bulk Heterojunction Solar Cells. *Adv. Energy*
493 *Mater.* **4,** (2014).
494 40. Carey, G. H. *et al.* Colloidal Quantum Dot Solar Cells. *Chem. Rev.* **115,** 12732–12763
495 (2015).
496 41. Mueller, C. J., Singh, C. R., Fried, M., Huettner, S. & Thelakkat, M. High Bulk
497 Electron Mobility Diketopyrrolopyrrole Copolymers with Perfluorothiophene. *Adv.*
498 *Funct. Mater.* **25,** 2725–2736 (2015).

42. Price, M. B. *et al.* Hot-carrier cooling and photoinduced refractive index changes in organic–inorganic lead halide perovskites. *Nat. Commun.* **6,** 8420 (2015).

Figure 1

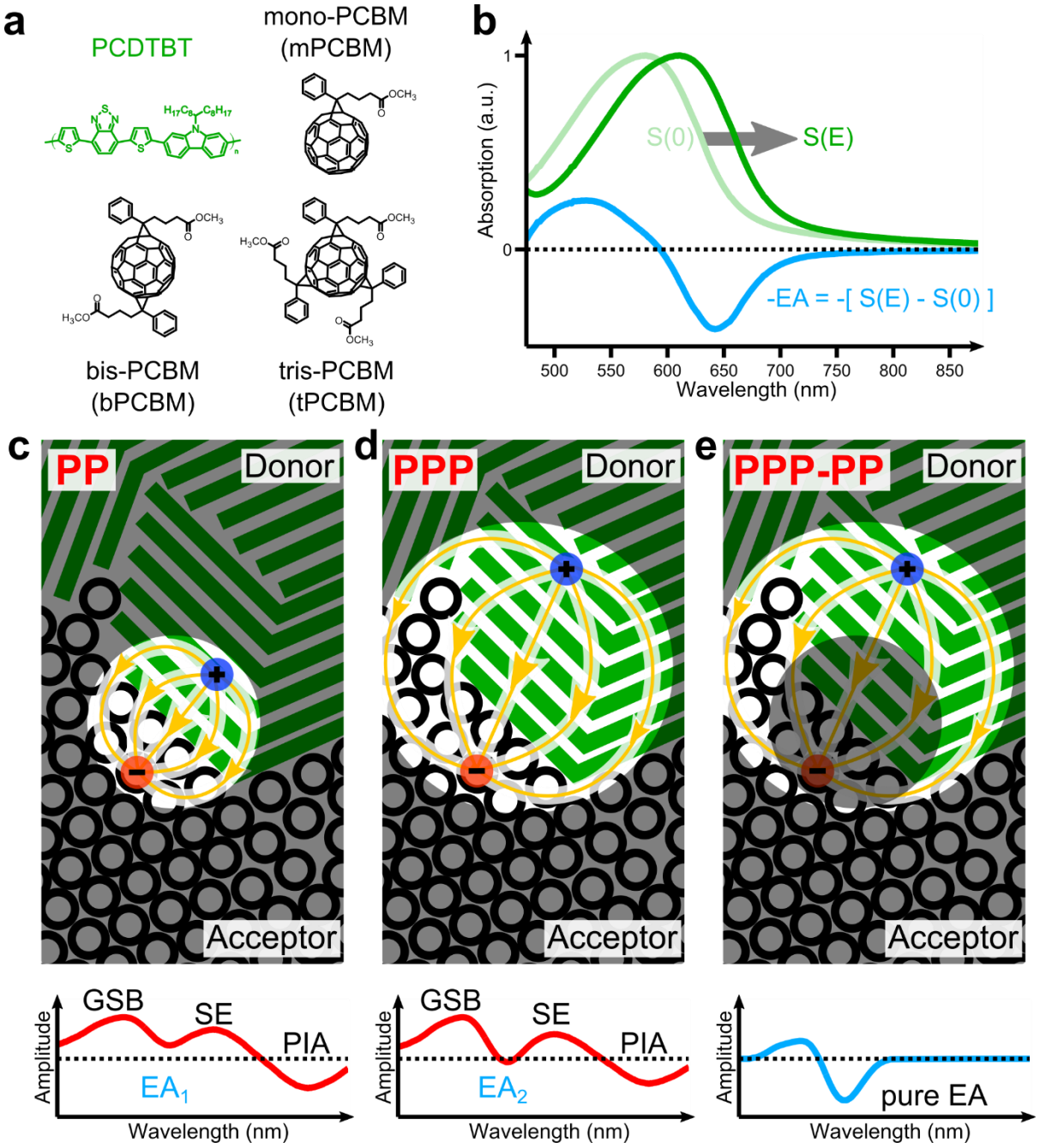

Figure 1: *Origin of the electroabsorption signal in pump-probe and pump-push-probe measurements.* ***(a)*** *Chemical structures of PCDTBT and PCBM fullerene acceptors.* ***(b)*** *Schematic origin of the spectral electroabsorption (EA) features due to a Stark shift of energy levels of the ground state absorption S(0) in the presence of an electric field S(E). The electric field shift is exaggerated to highlight the resulting spectrum, which is flipped in sign for better comparison with the feature observed in transient absorption.* ***(c)*** *States probed by*

pump-probe (PP) and a qualitative spectrum composed of the different components. Signals like the ground-state bleach (GSB), stimulated emission (SE) and photo-induced absorption (PIA) are specific to the site occupied by the charges. In contrast, the EA contains information from molecules in the volume influenced by the electric field, as shown by the brightened region. Only few electric field lines are shown and the extension to the 'outside' of the electron hole pair is omitted for simplicity reasons. The dotted line in the signal sketch represents the zero value of the signal amplitude. ***(d)*** *States probed by pump-push-probe (PPP) and a corresponding sketch of a qualitative spectrum. The push pulse moves the hole away from its original position. The electron-hole separation is increased and the electric field changed. Therefore, the EA signal is changed as indicated by the enlarged brightened area, while the site specific signals, such as GSB, SE and PIA are not changed as they still arise from the same electronic species (charges).* ***(e)*** *Subtraction of PP from the PPP, yields a small spatial area (indicated by the remaining brightened area) from which a pure EA signal of the area near the interface of the bulk-heterojunction can be retrieved.*

524 **Figure 2**

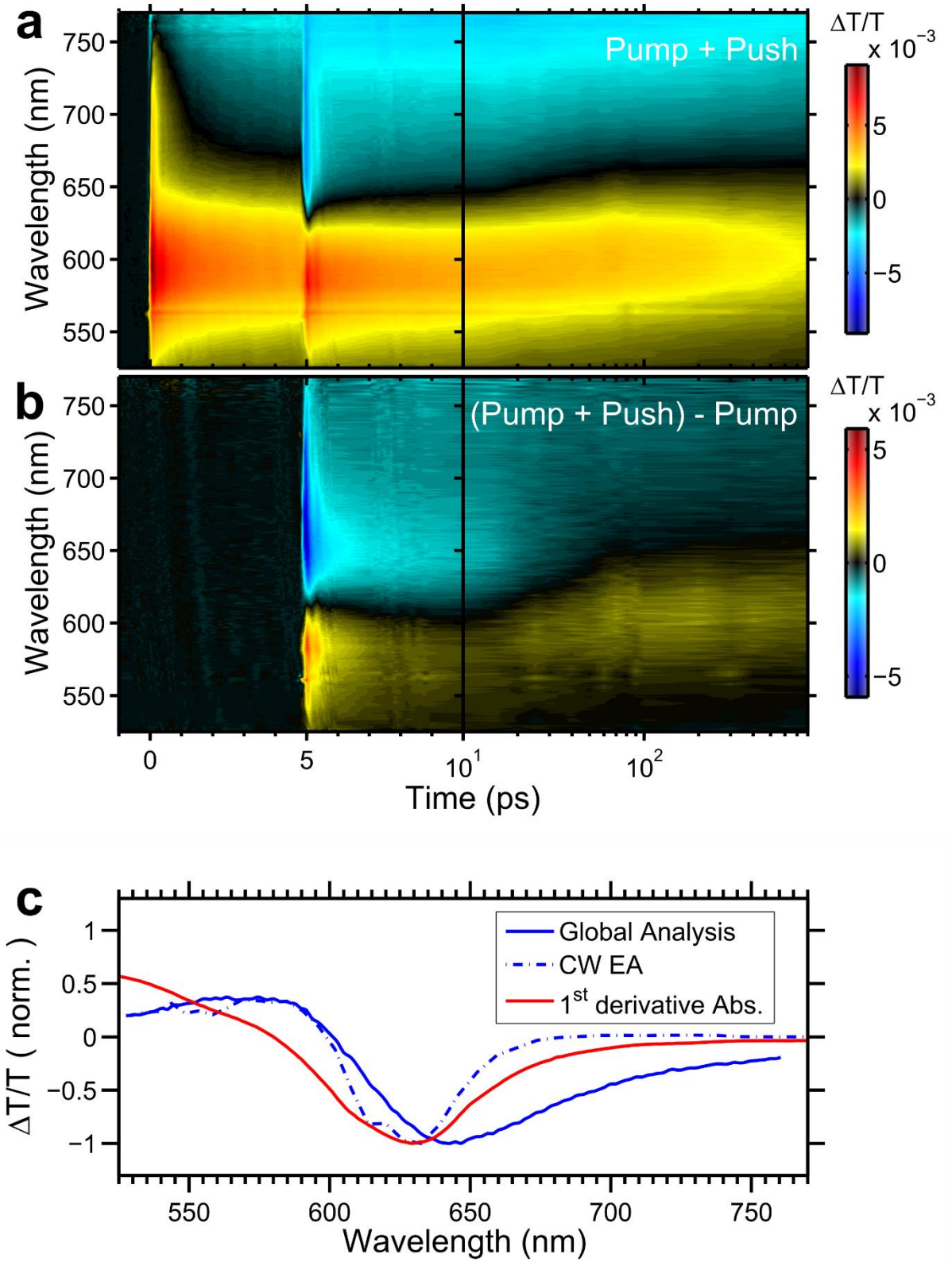

525

526 ***Figure 2****: Pump-push-probe data for PCDTBT:mono-PCBM (4:1) with 500 nm pump and*

527 *2000 nm push pulses arriving after 4.9 ps delay.* ***(a)*** *Full TA map with pump and push pulses*

present and ***(b)*** *the differential TA map between pump-push-probe and pump-probe revealing the influence of the push pulse only. We note that the direct sequence of pulses allows us to obtain data of high accuracy by purely subtracting the pump-probe dataset, as can be seen from the zero signal region for times smaller than 4.9 ps.* ***(c)*** *The main spectral component of a global analysis of this differential TA map, which is found to match the electroabsorption (EA) spectrum, alongside a reference spectrum from steady-state EA measurement (CW EA) and the first derivative of the absorption spectrum (red).*

Figure 3

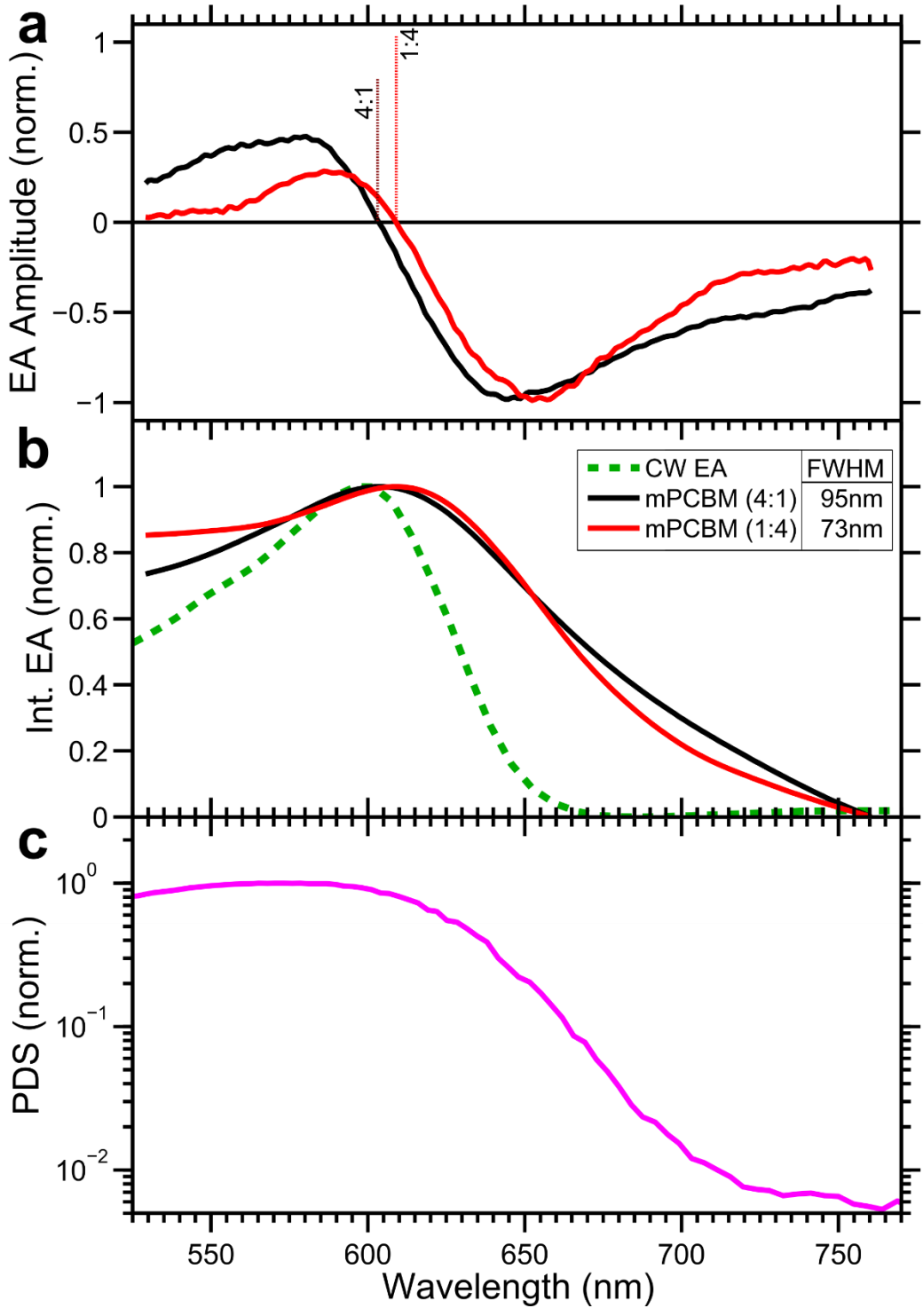

Figure 3: *Pump-push-probe measurements and resulting EA spectra on PCDTBT:mPCBM 4:1 (black) and 1:4 (red) blends.* ***(a)*** *EA spectra obtained from global analysis on the difference TA map between pump-push-probe and pump-probe datasets with the push pulse arriving 0.9 ps after initial excitation. These differential TA maps represent the pure impact*

of the push pulse. With the push not being absorbed by the ground state, the EA response arises only from moving hole-polarons via the push pulse. ***(b)*** *Integrated EA spectra from (a) including the integrated CW EA signal (green dashed line, measured on a diode under applied electrical field), which is indicative of the steady state absorption of the film. The column next to the legend shows the FWHM of a bi-Gaussian fit to the respective curve.* ***(c)*** *PDS spectra of a thin film of neat PDCTBT, giving insights into low energy tail states (note the log scale).*

548 **Figure 4**

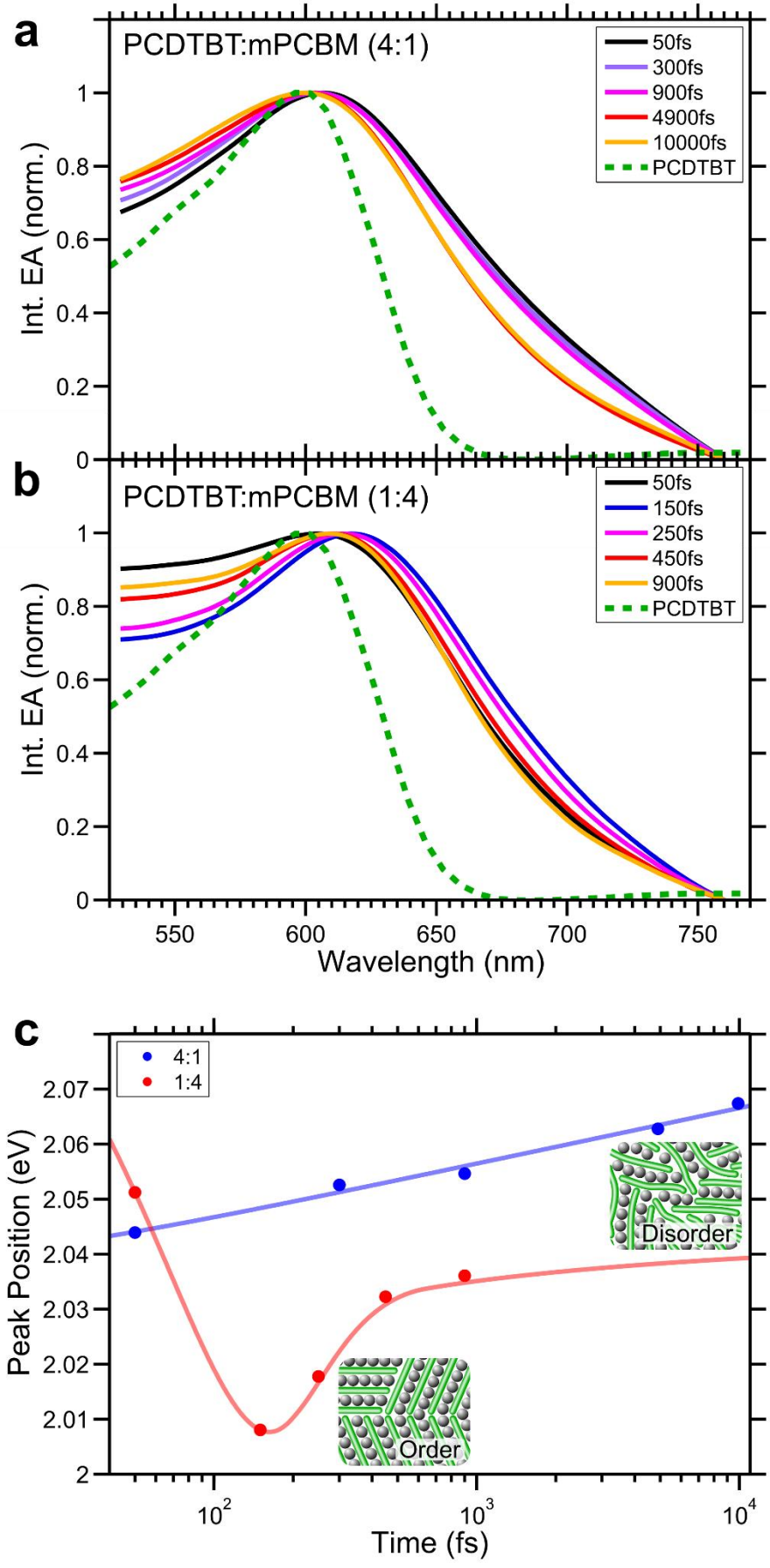

549

Figure 4: *Spectral signatures of charges moving through different material regions after the initial charge transfer step.* ***(a)*** *Integrated EA spectra obtained from global analysis on the differential TA map between pump-push-probe (PPP) and pump-probe (PP) datasets of the PCDTBT:mPCBM (4:1) blend. Spectra were recorded at different delays between pump and push pulses ranging from 50 fs to 10 ps. The integrated CW EA signal (green dashed line) is included to indicate the steady state absorption of the film.* ***(b)*** *Integrated EA spectra from global analysis on the PPP-PP differential map of the PCDTBT:mPCBM (1:4) composition. Here, time delays between pump and push pulses were varied between 50 fs and around 1 ps with more steps at earlier times due to the faster charge generation timescale. The integrated CW EA signal (green dashed line) is included to indicate the steady state absorption of the film.****(c)*** *Peak positions of integrated EA signals of 4:1 (blue symbols) and 1:4 (red symbols) PCDTBT:mPCBM blends with regard to the respective pump-push delays. While holes in the 4:1 blend slowly migrate to more disordered regions, in the 1:4 blends, they move into more ordered regions on 150fs timescales, followed by a slower movement into slightly more disordered regions. The solid lines are guides to the eye and the cartoons are show planar and disordered polymer chains. We note that they are not meant to represent the real morphology.*